

CHARACTERISTICS AND ENVIRONMENTAL RISKS OF THE OIL SHALE ASHES PRODUCED BY AEROBIC COMBUSTION AND ANAEROBIC PYROLYSIS PROCESSES

TAYEL EL-HASAN^{(a,b)*}

^(a) Department of Chemistry, Faculty of Science, Mu'tah University, 61710, Al-Karak, Jordan

^(b) Prince Faisal Center for Dead Sea, Environmental and Energy Researches, Al-Karak, Jordan

Abstract. *This study aimed to investigate the changes in oil shale (OS) ash as treated by the aerobic combustion process (ACP) and anaerobic pyrolysis process (APP). ACP ashes had all major oxides, and the trace elements content increased with burning temperature increasing up to 1000 °C. Meanwhile, APP ashes had a slight enrichment in V, Cr, Ni, Cu and U, but were depleted in As, Zn and Cd. No change in the ashes mineralogy was observed. X-ray absorption near edge structure (XANES) measurements showed that toxic elements converted from lower oxidation states into more mobile higher oxidation species such as Cr⁶⁺, As⁵⁺ and V⁵⁺. Moreover, the leaching test on ACP ashes gave alkaline elutes rich in Cr, i.e. 30 mg/L. Based on this result, the expected huge friable tailings produced would interact with rain water which might result in toxic elements-rich leachates, thus causing severe pollution.*

Keywords: *oil shale ash, leaching, aerobic combustion, anaerobic pyrolysis, enrichment factor, environmental risks.*

1. Introduction

Jordan has very large reserves of black shales, which are highly enriched with organic and inorganic matters. The largest deposits are found in the country's central region, mainly at El-Lajjun and Es-Sultani located 80–110 km south of Amman, with the average thickness of oil shale (OS) of about 30 m [1]. The oil shale geological reserves make up 1196 Mt and indicated reserves, 1170 Mt, with an average oil content of 10.5 w/w% and average total organic carbon (TOC) of about 22.1 w/w% [2].

* Corresponding author: e-mail tayel@mutah.edu

Lithologically oil shale belongs to the Upper Cretaceous-Paleocene. The organic geochemistry and oceanography of oil shale have been investigated by many researchers [3–5]. The author's previous work showed oil shale to have a high TOC content, in the range of 17.39–22% [6]. At the same time, the environmental impact of oil shale exploitation and industry has also been dealt with. In Jordan, the leachability tests done on oil shale showed that there would be substantial amounts of Ca, Mg, Na, K, Cl, SO₄, HCO₃, Fe, Cr, Cd and Pb as possible leachates that could reach surface and subsurface water resources [7]. Jordan pays much attention to the utilization of its organic-rich oil shale. However, OS utilization is expected to produce ash tailings. The combustion process generates large amounts of organic and inorganic matter that might be hazardous. This study will be concerned with ash/water interfaces resulting in the dissolution of high concentrations of organic and inorganic compounds contained in the ash. The dissolution of these compounds is a function of water temperature, pH, salinity, Eh, etc. The resulting solution or leachate is more likely to reach soil, plants, groundwater and surface water bodies, thus causing serious contamination. Novel technologies such as synchrotron radiation have proved to be useful in environmental implications. A recent study reported the release of Cr⁶⁺ up to 1 mmol/L from the oil shale aerobic combustion process (ACP) ashes treated with normal tap water [8]. The test was done according to the European compliance leaching test CEN/TC 292 EN 12457-1 (1:2 solid/water ratio, 24 hours shaking) [9].

The goal of this study was to carry out an assessment of environmental risks of oil shale combustion prior to launching industrial production. Thus, the proposed work is designed as a precautionary research. The detailed objectives are to investigate the chemical and mineralogical characteristics of the original oil shale, and the ashes produced by the aerobic combustion process (ACP) and anaerobic pyrolysis process (APP), and to determine the chemical characteristics of the effluent or leachate produced from these ashes.

2. Materials and analytical methods

2.1. Sample collection and ash sample preparation

Oil shale rock samples were collected from El-Lajjoun area, central Jordan (Fig. 1). The samples underwent crushing, grinding and sieving < 63 μm, and were homogenized. To prepare the ACP ashes sample, OS powder samples were divided into four fractions and placed in capped porcelain dishes. Three fractions of each sample were burned in the presence of oxygen at 700, 850 and 1000 °C, respectively, for four hours using a muffle furnace. The samples were allowed to cool down inside a desiccator and then kept in a sealed polyethylene bottle.

The anaerobic pyrolysis process was carried out by placing 300 g of the oil shale powder in a cylindrical glass retort and flushing it with nitrogen at a flow rate of 100 mL min⁻¹. During heat-up, the generated hydrocarbons were

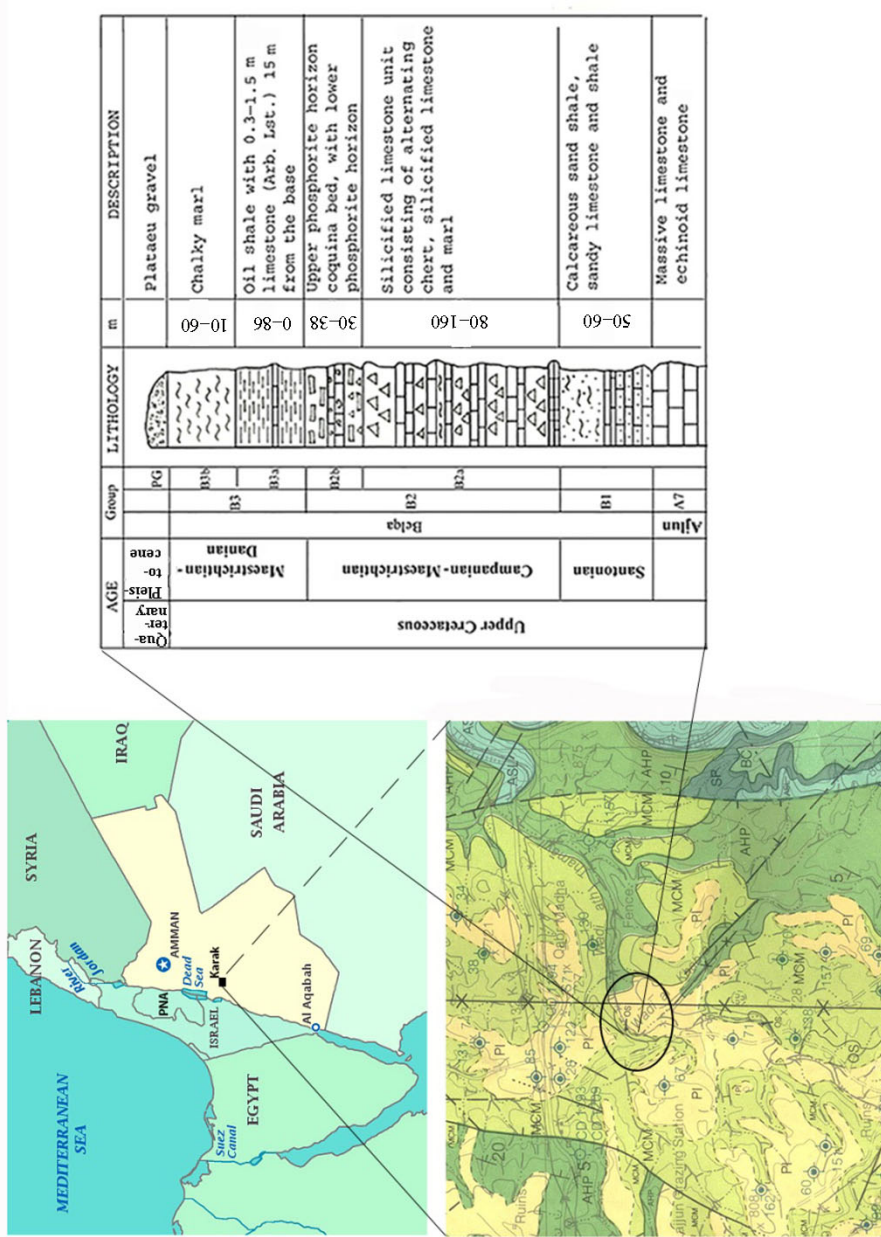


Fig. 1. Location map of the study area with a columnar section of the sampling outcrop.

passed into a water-cooled receiver. When the desired temperature set point was reached, the heater was switched off immediately, but the N₂ flow was maintained for cooling the retort down to 150 °C. The sample was then removed from the retort, cooled down to room temperature, weighted, and sealed in a polyethylene bottle. Five APP ashes samples were obtained at temperatures from 600 to 800 °C at 50 °C intervals. A temperature range beyond the common Fischer Assay (ISO 647) was chosen to cover the full succession in shale oil decomposition reactions from pyrobitumen over asphaltenes and carboids up to methane formation.

2.2. Mineralogical analysis

The mineral constituents of the samples were determined using Philips-X'pert MpD X-Ray Diffraction (XRD) system. The powder samples were scanned between 2 and 65°, using Ni-filtered Co K α -radiation, 40 kv/40 mA, 0.02° mm divergent and scattering slits, a 0.15 mm receiving slit, with a stepping of 0.01° and scanning speed of 3°/min.

2.3. Bulk elemental analysis of the original rock and ashes

Bulk geochemical analysis of OS and ACP and APP ashes was carried out using XRF. Sample pellets were prepared using a Herzog hydraulic press (Germany), in which fine powdered samples with a minor epoxy resin admixture were cast at 7-tonne pressure in a 30-mm direct-injection enthalpimeter (DIE). A Philips MagiX PRO wavelength dispersive X-ray spectrometer (WD-XRF) was used for the total concentration determination of major and trace elements. The MagiX PRO is a sequential instrument with a single goniometer based measuring channel equipped with a rhodium anode X-ray tube operated at 3.6 kW. The system analytical software Philips SuperQ V4.0 was used for data collection, calibration and analysis. The samples were run against a collection of international standard reference materials in the databank to prepare the calibration curves for major and trace elements and to assure the analytical accuracy. Synchrotron-based X-ray absorption near edge structure (XANES) measurements were done using the results reported earlier [8]. Loss-on-ignition (LOI) was determined using a muffle furnace at 1000 °C, which was weighted after cooling. Total organic carbon and sulfur (S) were determined using a LECO[®] combustion oven with an infrared detector on gas emissions. The relative error was less than $\pm 5\%$.

2.3.1. Elution test for ACP ashes

The elution test for the ACP ashes sample was done according to DIN 38414-4 [10] at Braunschweig Technical University. 5 g of the powder sample was suspended in 50 mL pure water. After 24 hours of shaking the sample pH was measured using a WTW pH 330i set (Germany), afterwards the sample was filtered through a polytetrafluoroethylene (PTFE)-membrane

filter, pore size 0.45 μm . The concentrations of major and trace elements were determined using inductively coupled plasma optical emission spectrometry (ICP-OES). The parameters of the Varian Vista-MPX ICP-OES (Germany), which consisted of a concentric glass nebulizer (SeaSpray nebulizer) and a glass cyclonic spray chamber were as follows: power 1.20 kW; plasma flow 15.0 LAr/min; auxiliary flow 1.50 L Ar/min; nebulizer pressure 40 PSI; replicate read time 20 sec; instrument stabilization delay 45 sec; sample uptake delay 45 sec; pump rate 20 upm; rinse time 20 sec; and the number of replicates 3; in fitted background correction mode. The elements content regulations were made by external calibrations. The calibration rows covered several calibration standards which were in the element concentration ranges between 0 and 500 mg/L. The standard solutions were prepared using single element solution standards of the concentration of 1,000 mg/L or 10,000 mg/L, Specpure®.

2.3.2. Elution test for APP ashes

APP ashes elutes were investigated for heavy metal release by using an Agilent 7700 ICP-MS machine model. Calibration was done using single element solutions with concentrations between 0 and 500 mg/L. Ground 0.4 g samples of APP ashes of 600 °C and 700 °C were covered with 50 mL deionized water in Erlenmeyer flask, and then shaken for 90 minutes at 130 RPM and 26 °C. Thereafter the decanted water was filtered and analyzed for releasing metals.

3. Results and discussion

3.1. Effect of burning process on ashes mineral composition

The mineralogical composition of the original oil shale was reported by El-Hasan [6] who showed that calcite was its main mineral phase, followed by quartz and apatite. The minor phases were kaolinite and gypsum. Besides, dolomite-hematite and pyrite were present as accessory minerals. The main effect of ACP on ash mineralogy was revealed in changing gypsum into the anhydrite phase whose intensity increased with increasing burning temperature up to 1000 °C, as shown in Figure 2a and reported previously [11].

Moreover, apatite also seemed to be enhanced in the ashes as its peak intensity rose with increasing burning temperature (Fig. 2a). The rapid aerobic burning decreased the replacement of Ca by P, which is evident from the presence of apatite in the ashes formed at 1000 °C. The intensity of burning of both calcite and quartz became much stronger in ashes at higher temperatures, i.e. 850 °C and 1000 °C. These results are in agreement with the fact that at higher temperatures, above 400 °C, calcite is more stable than its polymorph phase aragonite. XRD showed a sharp quartz peak with high intensity in the original rock; however, the peak intensity decreased with increasing burning temperature. This might be due to the phase changing

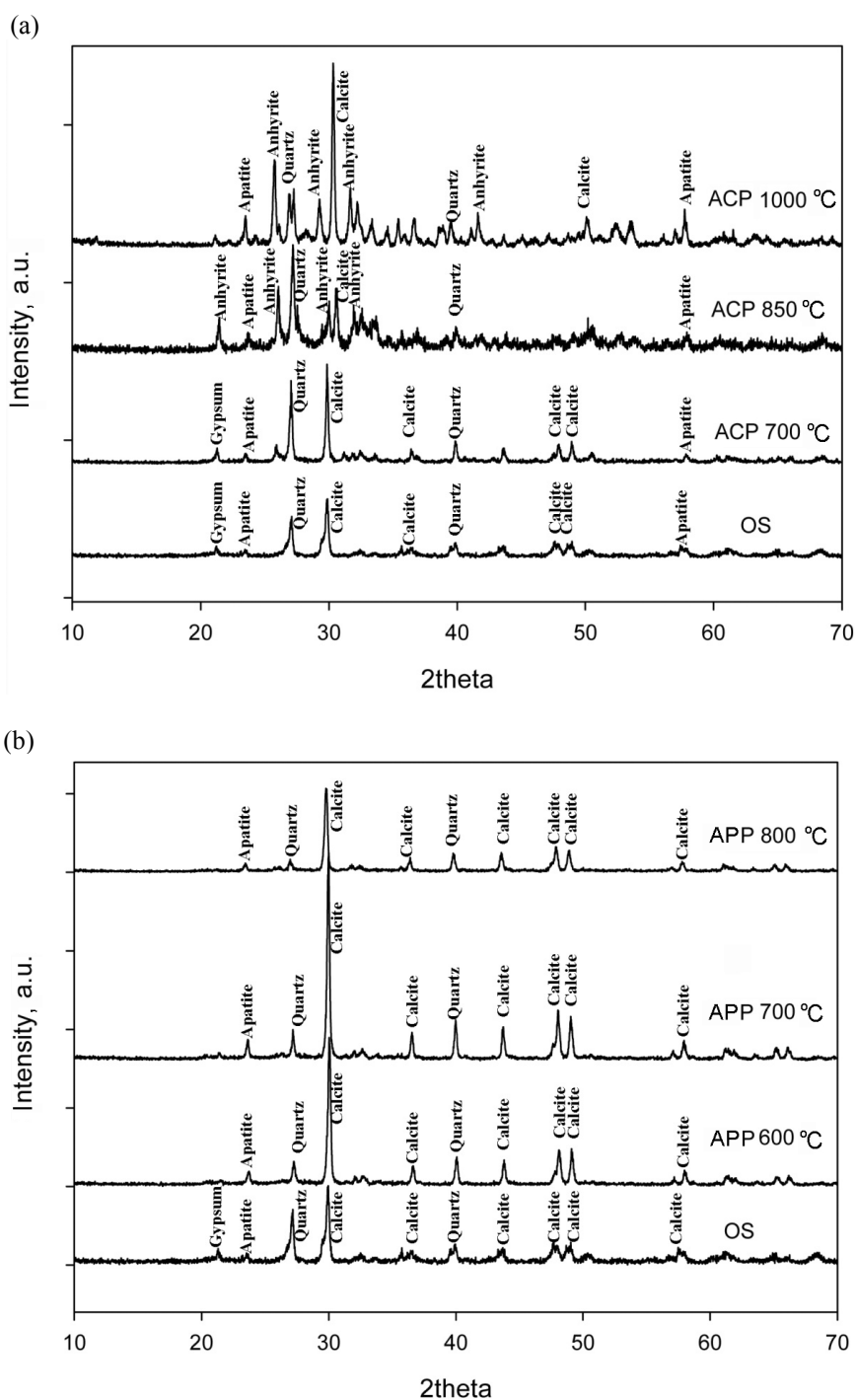


Fig. 2. (a) XRD chart for OS and 700 °C, 850 °C and 1000 °C ACP ashes; (b) XRD chart for OS and 600 °C, 700 °C and 800 °C APP ashes.

from α -quartz to β -quartz or β -tridymite. Such result is in accordance with the findings reported earlier [12]. The researchers found that at lower atmospheric pressure the stability field of quartz system started with the formation of α -quartz up to 573 °C, then β -quartz was produced at 573–870 °C, after that β -tridymite formed at 870–1470 °C, and above 1470 °C β -cristobalite was stable up to 1705 °C at which silica melted. The ACP ashes contained anhydrite, lime (“portlandite”) and minerals from the apatite and Ca-silicate groups, which characterizes them as moderately pozzolanic. This mineral assemblage fitted well with the geochemical analysis results, which revealed the increase in CaO and SiO₂ concentrations in the ashes at higher burning temperatures.

There was no significant difference in mineralogy between OS and APP ashes, only the weak peak of gypsum of OS vanished in the case of heated APP ashes, which might be due to the liberation of SO₄. However, unlike the ACP ashes, anhydrite was not detected. The peak of apatite became somewhat more distinct, beside the predominant sharp peaks of calcite and quartz, as shown in Figure 2b.

3.2. Effect of combustion processes on ashes bulk geochemistry

Elemental concentrations of ash samples are given in Tables 1 and 2. ACP affected the elemental contents in the produced ashes, especially that of SiO₂, which increased from 15.68 to 40.12 wt%. Also the CaO content increased, from 27.06 to 41.28 wt%. At the same time, the concentrations of other major oxides underwent but a slight to moderate increase. This was due to the loss on ignition, and of SO₃, which decreased from 42.92 to 1.37 wt%, and from 3.51 to 1.89 wt%, respectively. The total loss was 43 wt%, of which SiO₂ and CaO accounted for 90%, and other oxides, 10%.

As a result of ACP, the concentrations of all minor and trace elements in the ashes were also increased (Table 2). The contents of toxic and other elements increased as follows: Cu from 30 to 123 ppm, U from 15 to 42 ppm, Ni from 109 to 277 ppm, V from 156 to 318 ppm, Zn from 548 to 1013 ppm and Cr from 372 to 572 ppm (Table 2).

No significant difference in major oxides and trace elements contents between the ashes of 700 °C, 850 °C and 1000 °C was observed, which means that the threshold effect on ACP ashes was revealed already below 700 °C as shown in Figure 3a and b. The threshold effect is more likely to be revealed in the temperatures range in which kerogen is burned, i.e. 450–480 °C [13]. The conversion of kerogen upon retorting in the presence of CO and H₂O into soluble and gas materials begun at 350 °C, while the highest yields were obtained at 450 °C [14].

Enrichment factor (EF) was used to determine the rate of enrichment of trace elements in ACP ashes (Table 3). The data were normalized using the average EF of shale as reported in [15]. Al was used as a normalization element because the difference in its content between OS and APC ashes was the smallest. From the above it follows that the enrichment series of OS

Table 1. (a) Major oxides contents of OS and ACP ashes at different combustion temperatures, wt%; (b) Minor and trace elements contents of OS and ACP ashes at different combustion temperatures, ppm

(a)

	SiO ₂	Al ₂ O ₃	TiO ₂	Fe ₂ O _{3(t)}	CaO	MgO	Na ₂ O	K ₂ O	P ₂ O ₅	SO ₃	TOC	LOI
Oil shale	15.68	3.82	0.17	1.51	27.06	0.56	0.14	0.28	3.25	3.51	21.3	42.92
Ash 700 °C	34.95	4.18	0.2	1.72	36.09	1.23	0.14	0.53	4.45	2.77	3.88	14.83
Ash 850 °C	39.92	4.18	0.2	1.71	41.26	1.23	0.14	0.51	4.47	2.01	0.92	4.59
Ash 1000 °C	40.12	4.2	0.2	1.73	41.28	1.23	0.13	0.51	4.47	1.89	0.88	1.37

Note: TOC – total organic carbon, LOI – loss on ignition.

(b)

	As	V	Cr	Ni	Cu	Zn	Sr	Ba	U	Cd	Y	Zr	Sb	F	Cl	I
Oil shale	9	156	372	109	30	548	914	19	15	71	28	30	10	3204	895	183
Ash 700 °C	14	318	532	241	106	801	1086	71	37	83	32	49	10	4615	1011	165
Ash 850 °C	15	320	572	265	122	967	1231	79	41	94	35	55	11	4664	863	152
Ash 1000 °C	17	324	575	277	124	1013	1275	79	42	100	37	57	9	4657	864	146

Table 2. Major oxides contents of OS and APP ashes at different pyrolysis temperatures, wt%

	SiO ₂	Al ₂ O ₃	TiO ₂	Fe ₂ O _{3(t)}	CaO	MgO	Na ₂ O	K ₂ O	P ₂ O ₅	SO ₃	TOC	LOI
Oil shale	15.68	3.82	0.17	1.51	27.06	0.56	0.14	0.28	3.25	3.51	21.3	42.92
Ash 600 °C	18.95	5.8	0.277	2.61	57.83	0.89	0.03	0.36	4.07	7.53		
Ash 650 °C	19.18	5.9	0.277	2.67	57.44	0.92	0.03	0.32	4.07	7.74		
Ash 700 °C	19.11	5.87	0.27	2.64	58	0.92	0.06	0.33	4.08	7.47		
Ash 750 °C	18.94	5.79	0.271	2.62	57.81	0.9	0.03	0.34	4.08	7.41		
Ash 800 °C	19.97	6.25	0.292	2.84	56.5	0.96	0.05	0.39	4.01	7.23		

Note: TOC – total organic carbon, LOI – loss on ignition.

and ACP ashes were quite similar. For OS the series assumed the following order: Cd > Zn > Cr > U > Ni > V > As > Cu, while for ACP ashes of 700 °C it was Cd > U > Zn > Cr > Ni > V > Cu > As, for ACP ashes of 850 °C Cd > Zn > U > Cr > Ni > Cu > V > As; and for ACP ashes of 1000 °C Cd > Zn > U > Cr > Ni > Cu > V > As.

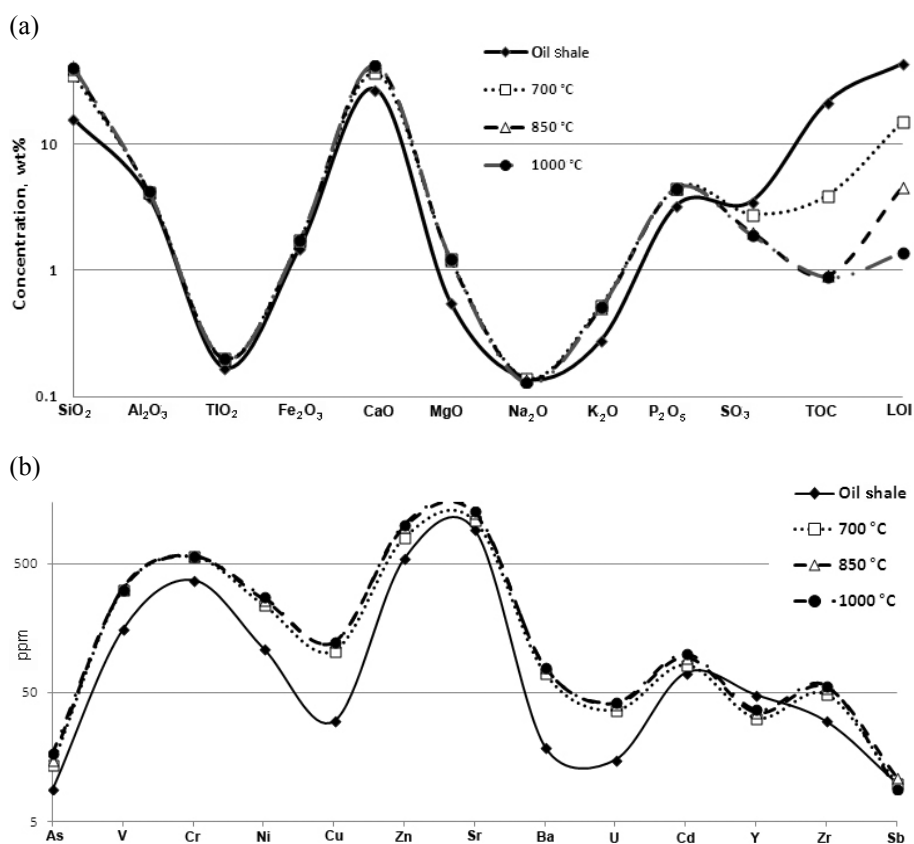


Fig. 3. (a) Bulk chemical analysis (major oxides) for OS and ACP ashes; (b) bulk chemical analysis (trace elements) for OS and ACP ashes.

Table 3. Enrichment Factor for trace elements in OS and ACP ashes, normalized based on average shale values (after [15])

	As	V	Cr	Ni	Cu	Zn	U	Cd
Oil shale	3.01	4.72	16.26	6.33	2.55	22.69	14.80	1032.35
Ash 700 °C	4.27	8.83	21.24	12.82	8.24	30.38	33.40	1088.24
Ash 850 °C	4.54	8.83	22.83	14.00	9.48	36.64	37.00	1247.06
Ash 1000 °C	5.15	8.90	22.65	14.64	9.60	38.24	37.80	1320.59
EF(OS/1000 °C)	0.59	0.53	0.72	0.43	0.27	0.59	0.39	0.78
EF(1000 °C/OS)	1.71	1.88	1.39	2.31	3.76	1.69	2.55	1.28

Only U and Cu concentrations were increased in ACP ashes. The most enriched elements in OS and the ashes were Cu, U and Ni, the OS/ACP ashes 1000 °C ratio being 3.76, 2.55 and 2.31, respectively. At the same time, V, As, Zn and Cr exhibited a slight enrichment, the respective ratio being 1.88, 1.71, 1.68 and 1.39. Obviously, the contents of lower-concentration elements in OS increased most, while those of higher-concentration ele-

ments experienced a moderate to slight increase. The above toxic elements were present in ACP ashes as free cations due to the breakdown of their mineral carriers or adsorbate by combustion. Toxic elements were mainly captured or adsorbed onto the sulphur and organic matter [6, 16]. The huge friable ash tailings might react with rain water and give leachates that may exert a harmful impact on the surrounding environment.

3.3. APP ashes geochemistry

There was no significant difference in enrichment series between the APP and ACP ashes, while both had higher contents of U and Cu, and lower contents of Zn and As than OS (Table 4). However, comparison of the EFs of OS, ACP ashes 1000 °C and APP ashes 800 °C revealed that the ACP ashes were highly enriched in all toxic elements, while in the APP ashes there was but a slight enrichment of V, Cr, Ni, Cu and U, and depletion of As, Zn and Cd (Fig. 4). This might be attributed to the fact that As and Cd were vaporized during anaerobic retorting. An earlier study showed that

Table 4. Enrichment Factor for trace elements in OS and APP ashes, normalized based on average shale values (after [15])

	As	V	Cr	Ni	Cu	Zn	U	Cd
OS	3.01	4.72	16.26	6.33	2.55	22.69	14.80	1032.35
Ash 600 °C	2.64	5.21	17.65	7.42	4.49	9.43	17.05	66.98
Ash 650 °C	2.6	5.18	16.92	7.22	4.52	9.73	18.68	47.03
Ash 700 °C	2.61	5.17	17.15	7.34	4.54	10.37	18.32	56.72
Ash 750 °C	2.65	5.32	17.79	8.01	5.28	10.63	19.62	38.34
Ash 800 °C	2.66	5.17	16.51	7.32	4.58	9.28	17.33	71.03
EF(OS/800 °C)	1.13	0.91	0.98	0.87	0.56	2.44	0.85	14.53
EF (800 °C/OS)	0.88	1.09	1.02	1.16	1.8	0.41	1.17	0.07

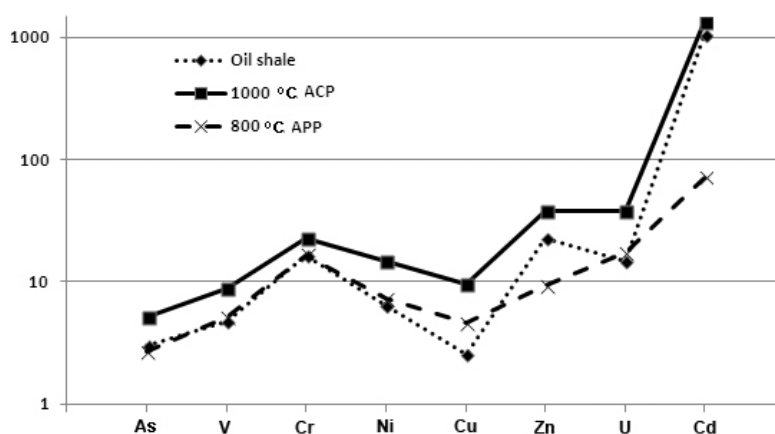


Fig. 4. Plots of EF of trace and toxic elements for OS, ACP and APP ashes.

arsine gas was trapped during retorting following the Fischer Assay procedure [17]. The researchers established that As was converted into gaseous arsine as retorting was carried out under reducing conditions, i.e. pyrolysis. Consequently, neither As nor Cd was found in the retorting water. At the same time, other toxic elements such as Cu, Zn, Cr, Pb, Ni and V were detected [18–21].

3.4. Elution test results

The elemental leachability potential of ACP ashes of the three temperatures was investigated. The elutes were alkaline (pH 12) and were enriched in Ca, S, Na, K, Sr and Cr. The average concentration of Cr was 30 mg/L (Table 5). Metal release from APP ashes samples was very low (Table 6). This might be due to the use of deionized water which is a rather weak solute.

Table 5. Elemental concentrations of elutes from ACP ashes

Sample Element	Elute 700 °C, mg/L	Elute 850 °C, mg/L	Elute 1000 °C, mg/L
Al	< 1	< 1	< 1
Ca	2,970	1,460	1,870
Cd	< 1	< 1	< 1
Co	< 1	< 1	< 1
Cr	27.3	35.6	29.1
Cu	< 1	< 1	< 1
Fe	< 1	< 1	< 1
K	19.8	23.5	14.1
Mg	< 1	< 1	< 1
Mn	< 1	< 1	< 1
Na	38.4	21.0	14.6
Ni	< 1	< 1	< 1
P	< 1	< 1	< 1
Pb	< 1	< 1	< 1
S	869	503	681
Sr	19.2	10.4	7.73
Ti	< 1	< 1	< 1
Zn	< 1	< 1	< 1
pH	11.5	12.4	12.3

Table 6. Elemental concentrations of elutes from APP ashes

Metal	Oil shale 600 °C, ppb	Oil shale 700 °C, ppb
Cr	≤ 0.07	≤ 0.07
Fe	≤ 0.07	≤ 0.07
Co	≤ 0.01	≤ 0.01
Ni	≤ 0.01	≤ 0.01
Cu	≤ 0.06	≤ 0.06
Zn	2.1	2.2
As	≤ 0.01	≤ 0.01
Cd	≤ 0.06	≤ 0.06
Pb	≤ 0.09	≤ 0.09
pH	11.8	12.4

The depletion of other toxic elements in the elution solution was probably controlled by the high pH which decreased its solubilizing potential. These findings compare well with those reported earlier by other investigators [21, 22]. However, in the area of oil shale mining and combustion, considerable gas emissions, especially sulfur, would be produced. This will decrease the pH of rainwater and eventually make the medium neutral. Therefore, rainwater interacts with friable ash tailings and cause the generation of many toxic elements to be dissolved and mobilized.

The oxidation states of elements in OS and ACP ashes were determined using XANES. It was found that Cr and As in the oxidation states Cr^{+3} and As^{+3} in OS were converted to Cr^{+6} and As^{+5} in ACP ashes, respectively (Fig. 5a). The conversion into higher oxidation states increased with increasing combustion temperature (Fig. 5b) [8].

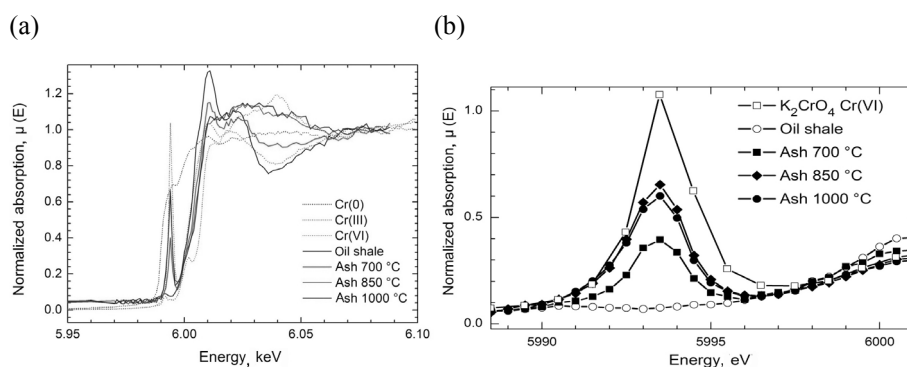


Fig. 5. (a) Cr^{3+} and Cr^{6+} and their standard pre-edge XANES curves (after [8]); (b) Cr K-edge XANES analysis for OS and ACP ashes (after [8]).

4. Conclusions

Both the aerobic combustion and anaerobic pyrolysis processes significantly increased the concentrations of major oxides and trace elements in the ashes, compared to OS, with increasing burning temperature, due to the loss of organic matter during burning. The enrichment factor showed that the aerobic combustion process influenced the ashes composition a lot more than the anaerobic pyrolysis process, causing the enrichment of its ashes in toxic elements. The X-ray absorption near edge structure measurements established that all elements were present in higher oxidation states, meaning higher mobility and involving thus a higher pollution risk to surface and groundwater bodies. The leaching test performed on ACP and APP ashes indicated that the former leached Cr^{6+} easily, 30 mg/L on average. Therefore, it is highly recommended to keep the huge ACP ashes tailings in well-designed landfill sites, and solidify them.

Acknowledgments

This work was done through Mu'tah University sabbatical leave scholarship. The author is grateful to Prof. Michael Kersten, Mainz University, for carrying out XRF analysis, and to Prof. Mufit Bahadeir, Braunschweig Technical University (BTU), for performing the elution test. The author is deeply thankful to Bundesanstalt für Materialforschung und -prüfung (BAM) staff at Berliner Elektronenspeicherring-Gesellschaft für Synchrotronstrahlung (BESSY II-Berlin) for doing the synchrotron XANES analysis. Dr. Omar Al-Ayed at BTU is greatly acknowledged for carrying out the anaerobic pyrolysis combustion of oil shale. Thanks are also due to Dr. Abdulaziz Amro, Department of Chemistry, Taibah University, for the help in performing the elution test.

REFERENCES

1. Abu-Ajameiah, M. *An Assessment of the El-Lajjoun Oil Shale Deposit*. Unpublished report NRA, Amman, Jordan, 1980.
2. Hamarneh, Y. *Oil Shale Resources Development in Jordan*. NRA, Amman, Jordan, 1998.
3. Al-Nimry, Y., Abu-Ajamieh, M., Omari, K., Daghestani, F., Hamarneh, Y. *Oil Shale in Jordan*. Unpublished report, NRA, Amman, Jordan, 1981.
4. Klöckner Industrieanlagen GmbH. *Full-Fledged Feasibility Study 50,000 BBL/D Retorting Complex El-Lajjuon*. Unpublished final test report, Amman, Jordan, 1988.
5. Bechtel National Inc. *Prefeasibility Study, Oil Shale Utilization for Power Production in Jordan (HKJ)*. Unpublished report 89-02, NRA, Amman, Jordan, 1989.
6. El-Hasan, T. Geochemistry of the redox-sensitive trace elements and its implication on the mode of formation of the Upper Cretaceous oil shales, Central Jordan. *Neues Jahrb. Geol. P-A.*, 2008, **249**(3), 333–344.
7. Al-Harashsheh, A., Al-Adamat, R., Al-Farajat, M. Potential impacts on surface water quality from the utilization of oil shale at Lajjoun Area/Southern Jordan using geographic information systems and leachability tests. *Energy Sources A*, 2010, **32**, 1763–1776.
8. El-Hasan, T., Szczerba, W., Buzanich, G., Radtke, M., Riesemeier, H., Kersten, M. Cr(VI)/Cr(III) and As(V)/As(III) ratio assessments in Jordanian spent oil shale produced by aerobic combustion and anaerobic pyrolysis. *Environ. Sci. Technol.*, 2011, **45**(22), 9799–9805.
9. CEN/TC 292 – EN 12457-1:2002. *Characterization of waste – Leaching – Compliance test for leaching of granular waste materials and sludges. Part 1*, 2002.
10. DIN 38414-4. *German standard methods for the examination of water, waste water and sludge – Sludge and sediments (Group S)*, 1984.
11. Rolnick, L. S. *The Stability of Gypsum and Anhydrite in the Geologic Environment*. Ph.D. Thesis, The Johns Hopkins University, 1950.
12. Wenk, H.-R., Bulakh, A. *Minerals – Their Constitution and Origin*. Cambridge University Press, Cambridge, 2004.

13. Hubbard, A. B., Robinson, W. E. *A Thermal Decomposition Study of Colorado Oil Shale*. Report of Investigations No. 4744, United States Bureau of Mines, US Department of the Interior, Washington, DC, 1950.
14. Cummins, J. J., Robinson, W. E. Thermal conversion of oil-shale kerogen in the presence of carbon monoxide and water. *Preprint Paper: Am. Chem. Soc., Div. Fuel Chem.*, 1976, **21**(6), 94–109.
15. Turkian, K., Wedpohl, K. H. Distribution of the elements in some major units of the earth's crust. *Bull. Geol. Soc. Am.*, 1961, **72**(2), 175–191.
16. Alego, T. J., Maynard, J. B. Trace-element behavior and redox facies in core shales of Upper Pennsylvanian Kansas-type cyclothems. *Chem. Geol.*, 2004, **206**(3–4), 289–318.
17. Shendrikar, A. D., Faudel, G. B. Distribution of trace metals during oil shale retorting. *Environ. Sci. Technol.*, 1978, **12**(3), 332–334.
18. Fox, J. P. *The Partitioning of Major, Minor and Trace Elements during Simulated In-Situ Oil Shale Retorting*. Ph.D. Thesis, University of California, Berkeley, 1979.
19. Fruchter, J. S., Wilkenson, C. L., Evans, J. C., Sanders, R. W., Abel, K. W. *Source Characterization Studies at the Paraho Semiworks Oil Shale Retort*. Battelle, Pacific Northwest Laboratory Report PNL-2945, 1979.
20. Bates, E. R., Thoem, T. L. Solid waste impacts (Environmental Protection Agency Report EPA-600/2-80-205a). In: *Environmental Perspective on the Emerging Oil Shale Industry* (Bates, E. R., Thoem, T. L., eds.). EPA Oil Shale Research Group, Cincinnati, Ohio, 1980.
21. Al-Harahsheh, M., Al-Ayed, O., Robinson, J., Kingman, S., Al-Harahsheh, A., Tarawneh, K., Saeid, A., Barranco, R. Effect of demineralization and heating rate on the pyrolysis kinetics of Jordanian oil shales. *Fuel Process. Technol.*, 2011, **92**(9), 1805–1811.
22. Al-Harahsheh, A., Al-Otoom, A., Al-Harahsheh, M., Allawzi, M., Al-Adamat, R., Al-Farajat, M., Al-Ayed, O. The leachability propensity of El-Lajjun Jordan oil shale ash. *Jordan Journal of Earth and Environmental Sciences*, 2012, **4**(2), 29–34.

Presented by V. Lahtvee

Received October 31, 2016